



[¹⁷⁷Lu]Lu-DOTA-TATE and [¹³¹I]MIBG Phenotypic Imaging-Based Therapy in Metastatic/Inoperable Pheochromocytomas and Paragangliomas: Comparative Results in a Single Center

Stefan Prado-Wohlwend^{1*}, María Isabel del Olmo-García², Pilar Bello-Arques¹ and Juan Francisco Merino-Torres^{2,3}

¹ Nuclear Medicine Department, University and Polytechnic Hospital La Fe, Valencia, Spain, ² Endocrinology and Nutrition Department, University and Polytechnic Hospital La Fe, Valencia, Spain, ³ Medicine Department, Universitat de València, Valencia, Spain

OPEN ACCESS

Edited by:

Piero Ferolla,
Umbria Regional Cancer Network, Italy

Reviewed by:

Annibale Versari,
IRCCS Local Health Authority of
Reggio Emilia, Italy
Ettore Seregni,
National Cancer Institute Foundation
(IRCCS), Italy

*Correspondence:

Stefan Prado-Wohlwend
prado_ste@gva.es

Specialty section:

This article was submitted to
Cancer Endocrinology,
a section of the journal
Frontiers in Endocrinology

Received: 16 September 2021

Accepted: 10 January 2022

Published: 07 February 2022

Citation:

Prado-Wohlwend S,
del Olmo-García MI, Bello-Arques P
and Merino-Torres JF (2022)
[¹⁷⁷Lu]Lu-DOTA-TATE and [¹³¹I]MIBG
Phenotypic Imaging-Based
Therapy in Metastatic/Inoperable
Pheochromocytomas and
Paragangliomas: Comparative
Results in a Single Center.
Front. Endocrinol. 13:778322.
doi: 10.3389/fendo.2022.778322

Purpose: The aim of the study is to assess phenotypic imaging patterns and the response to treatment with [¹⁷⁷Lu]Lu-DOTA-TATE and/or [¹³¹I]MIBG in paragangliomas (PGLs) and pheochromocytomas (PHEOs), globally and according to the primary location.

Methods: This is a 17-patient retrospective observational study, with 9 cases treated with [¹⁷⁷Lu]Lu-DOTA-TATE and 8 with [¹³¹I]MIBG (37 total treatments). Functional imaging scans and treatment responses were studied in order to choose the best therapeutic option and to define the progression-free survival (PFS) and disease control rate (DCR) according to treatment modality and primary location.

Results: All patients were studied with phenotypic nuclear medicine images. Twelve of 17 patients were tested with both [¹²³I]MIBG and somatostatin receptor images, and 6/12 showed appropriate expression of both targets to treatment in the phenotypic images. The rest of the patients were tested with one of the image modalities or only showed suitable uptake of a single radiotracer and were treated with the corresponding therapeutic option. [¹⁷⁷Lu]Lu-DOTA-TATE PFS was 29 months with a DCR of 88.8%. [¹³¹I]MIBG PFS was 18.5 months with a 62.5% DCR. According to the primary location, the best PFS was in PHEOs treated with [¹⁷⁷Lu]Lu-DOTA-TATE. Although the series are small due to the low disease prevalence and do not allow to yield statistically significant differences, this first study comparing [¹⁷⁷Lu]Lu-DOTA-TATE and [¹³¹I]MIBG displays a trend to an overall longer PFS with [¹⁷⁷Lu]Lu-DOTA-TATE, especially in the adrenal primary location. When both radionuclide targets are expressed, the patients' comorbidity and treatment effectiveness should be valued together with the intensity uptake in the phenotypic image in order to choose the best therapeutic option. These preliminary retrospective results reinforce the need for a prospective, multicentric trial to be confirmed.

Keywords: paraganglioma, pheochromocytoma, [¹³¹I]MIBG, PRRT, [⁶⁸Ga]Ga-DOTA-TOC, phenotypic imaging, [¹⁷⁷Lu]Lu-DOTA-TATE

INTRODUCTION

Paragangliomas (PGLs) and pheochromocytomas (PHEOs) collectively abbreviated as PGGLs are infrequent neuroendocrine tumors derived from chromaffin cells of the adrenal medulla and extra-adrenal sympathetic or parasympathetic ganglia that can be located from the skull to the sacrum.

Within this group, the term PHEO is reserved for a PGL derived from the adrenal medulla. Of PGGLs, 80%–85% are PHEOs, and approximately 15%–20% are PGLs (1). Most PGGLs related to the sympathetic nervous system secrete catecholamines (85%) in contrast to most PGGLs derived from the parasympathetic, which are mostly non-functioning.

The yearly incidence of overall PGGLs is between 1 and 2 cases per million, out of which 5%–20% of PHEOs and 15%–35% of PGLs present an advanced stage of the disease. Approximately 5%–10% are solitary, and the presence of metachronous or synchronous extra-adrenal PGLs is associated with germline or somatic mutations. PGGLs have a significant hereditary predisposition, with 30%–40% of them determined by a germinal autosomal dominant mutation. Depending on the mutation, they will show a specific phenotypic pattern in the images (2). So far, 32 genes related to this disease have been identified. SDHx are the most frequent mutations among metastatic PGGLs in adults (43%–71%) and children (70%–82%), followed by VHL mutations (1%–13%), whereas the cumulative frequency of RET, NF1, TMEM₁₂₇, and MAX is reported to be between 1% and 11% (3).

In patients with advanced disease, the goal of therapy is to reduce the tumor burden and to control the symptoms. In this context, the nuclear medicine theranostic radiopharmaceuticals play an important role in personalized health strategies, tailoring diagnosis and treatment for each patient and creating an emerging clinical dilemma to select the most suitable targeted radionuclide therapy (4, 5).

In order to solve this question, nuclear medicine phenotypic images are able to reveal tumor characteristics at the molecular and genetic levels reflecting the expression of certain target receptors or transporters (6).

The two main systemic available radiolabeled therapies in PGGLs are [¹⁷⁷Lu]Lu-DOTA-TATE, also called peptide receptor radionuclide therapy (PRRT), which binds to somatostatin receptors (SSTRs), and [¹³¹I]MIBG, which targets the norepinephrine transporter system (NET) (Figure 1).

[¹⁷⁷Lu]Lu-DOTA-TATE contains a semisynthetic somatostatin analog (SSA) with high affinity particularly for SSTR subtype 2 (SSTR2), bound through to a beta emitter ¹⁷⁷Lu isotope. This radiopharmaceutical binds to SSTR2s, which are overexpressed in at least 80% of the neuroendocrine tumors, enters within tumor cells, and is stored in the lysosomes, thereby causing cellular death by breaking DNA strands.

[¹³¹I]MIBG (low-specific-activity (LSA) MIBG) is a norepinephrine analog and adrenergic neuron blocker agent that enters neuroendocrine cells in two ways: a specific NET-mediated one with a high affinity and a passive diffusion mechanism with low affinity. Inside the cell, [¹³¹I]MIBG is

stored *via* vesicular monoamine transporter (VMAT) in neuroendocrine vesicles emitting beta particles.

To select whether to administer one or another radiolabeled treatment, the phenotypic nuclear medicine images signal the expression of the therapeutic targets. A patient can display appropriate uptake of one or both radiotracers, and in the latter scenario, the uptake can show a heterogeneous pattern, increasing the complexity of the therapeutic decision. In addition to the phenotypic images, we must also assess the patient's profile (age, previous treatment, and bone marrow reserve) and the characteristics of the tumor (volume, location, hormonal secretion, and growth rate), so as to choose the best treatment option (Figure 2).

MATERIAL AND METHODS

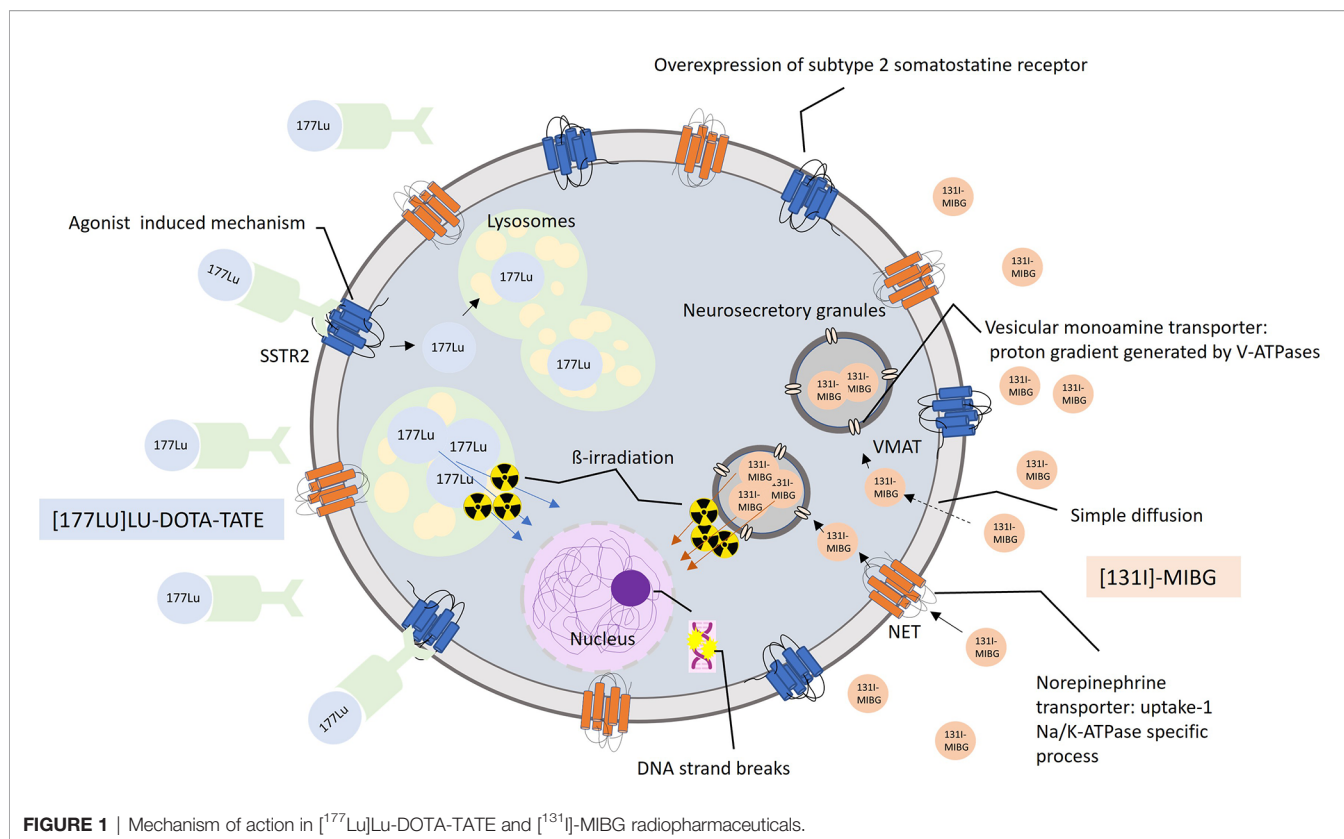
The primary aim of this report is to study the response to treatment in terms of progression-free survival (PFS) and disease control (DC) rate (DCR), with [¹⁷⁷Lu]Lu-DOTA-TATE and/or [¹³¹I]MIBG in PGLs and PHEOs, globally and according to the primary location. The secondary aim is to assess the phenotypic imaging-based selection to treatment and to evaluate which patients were candidates for both treatments.

This is a retrospective observational study involving 17 patients with histologically proven metastatic and/or inoperable PHEOs and PGLs, referred to our hospital for radionuclide therapy from April 2014 until May 2021. Nine patients were treated with PRRT and 8 with [¹³¹I]MIBG. A total of 37 treatment cycles were performed (28 PRRT and 9 [¹³¹I]-MIBG). A multidisciplinary committee evaluated the patients' medical history, radiological findings, tumor burden, and nuclear imaging studies in order to decide the best therapeutic option/target. The medical history was reviewed to classify in which treatment line the radionuclide therapy was administered. Phenotypic nuclear medicine and conventional imaging studies assessed the tumor burden.

The diagnostic phenotypic studies included in this report and performed at least 2 months prior to radionuclide treatment were as follows: [¹²³I]MIBG SPECT/CT, [¹¹¹In]In-Pentetreotide/[^{99m}Tc]Tc-HYNIC-TOC SPECT/CT (on the whole SSTR SPECT/CT), [⁶⁸Ga]Ga-DOTA-TOC PET/CT or PET/MRI (⁶⁸Ga-DOTA-SSA), [¹⁸F]fludeoxyglucose PET/CT ([¹⁸F]FDG) and L-6-[¹⁸F]fluorodopa PET/CT ([¹⁸F]DOPA). We reviewed whether nuclear medicine images assessed the possibility to treat with only one or both therapies, and their target phenotypic pattern (transporters/receptors intensity uptake, heterogeneity, and extension). The target and purpose of the scans are summarized in Table 1.

According to the radiotracers' uptake and its intensity, the patients were referred to PRRT, [¹³¹I]MIBG, or other non-radiolabeled systemic treatments with 4 possible scenarios:

1. Patients with obvious higher SSTR expression in ⁶⁸Ga-DOTA-SSA or SSTR SPECT/CT were referred to treatment with PRRT.



2. Patients with similar/higher [¹²³I]MIBG uptake than SSTR studies were referred to [¹³¹I]MIBG.
3. Heterogeneous or unclear better uptake pattern between SSTR images and [¹²³I]MIBG. In this scenario, the multidisciplinary committee decided the best approach depending on the phenotypic images, the patient's profile, and tumor features.
4. The cases with increased [¹⁸F]FDG uptake compared to the rest of radiotracers (especially lesions with glucose uptake and without SSTR or NET expression) were referred to other systemic treatments and were not included in this observational study.

We reviewed the functional imaging scans findings, prior systemic treatments, the genetic profile, and overall, clinical, hormonal, and radiological responses (the last one according to response evaluation criteria in solid tumors (RECIST) (7). PFS from the date of first radionuclide therapy until the last control or progression, DCR (patients with a response and disease stability), and follow-up until death or last available control were calculated. Contingency and multiparametric tests were performed on the variables under study. The contingency coefficient between PFS, therapeutic modality, previous treatments, and tumor location was evaluated, and statistical significances between them were assessed by the Mann–Whitney U test in those variables in which the samples were not dependent. The Kaplan–Meier survival plots were obtained (IBM SPSS Statistics 23).

Peptide Receptor Radionuclide Therapy

This group involved 9 patients (5 women) with a mean age of 45.8 years (20–72 years). Inclusion criteria were a tumor uptake higher than liver reference activity (Krenning score 3–4) in SSTR molecular imaging studies, blood test values according to international guidelines, life expectancy over 6 months, and Eastern Cooperative Oncology Group (ECOG) scale <2. No patient had relative or absolute contraindications prior to therapy (8).

Possible drug interferences were reviewed to avoid medication interactions. Long-half-life SSAs were withdrawn for 4–6 weeks before therapy and short-half-life formulations at least 24 h before treatment. Premedication with alpha- and beta-adrenergic drugs was considered in those patients with increased catecholaminergic symptoms.

Patients were admitted to the metabolic therapy unit for 24 h. An ondansetron premedication was administered firstly, followed by an amino acid infusion (2.5% lysine and 2.5% arginine) in 1 L of water, followed by the [¹⁷⁷Lu]Lu-DOTA-TATE radiopharmaceutical infusion over 30 min. The amino acid infusion was extended for 3 h after [¹⁷⁷Lu]Lu-DOTA-TATE. Standard administered activity was approximately 8.01 GBq per cycle (7.4–8.4) (SD 0.23) at a mean of 73.8 days' intervals (50–246 days) (SD 45.8).

Complete blood tests were performed 2, 4, and 6 weeks after each cycle and 6 months after therapy. Toxicities were described according to Common Terminology Criteria for Adverse Events version 5.0. Clinical follow-up assessed the response parameters.

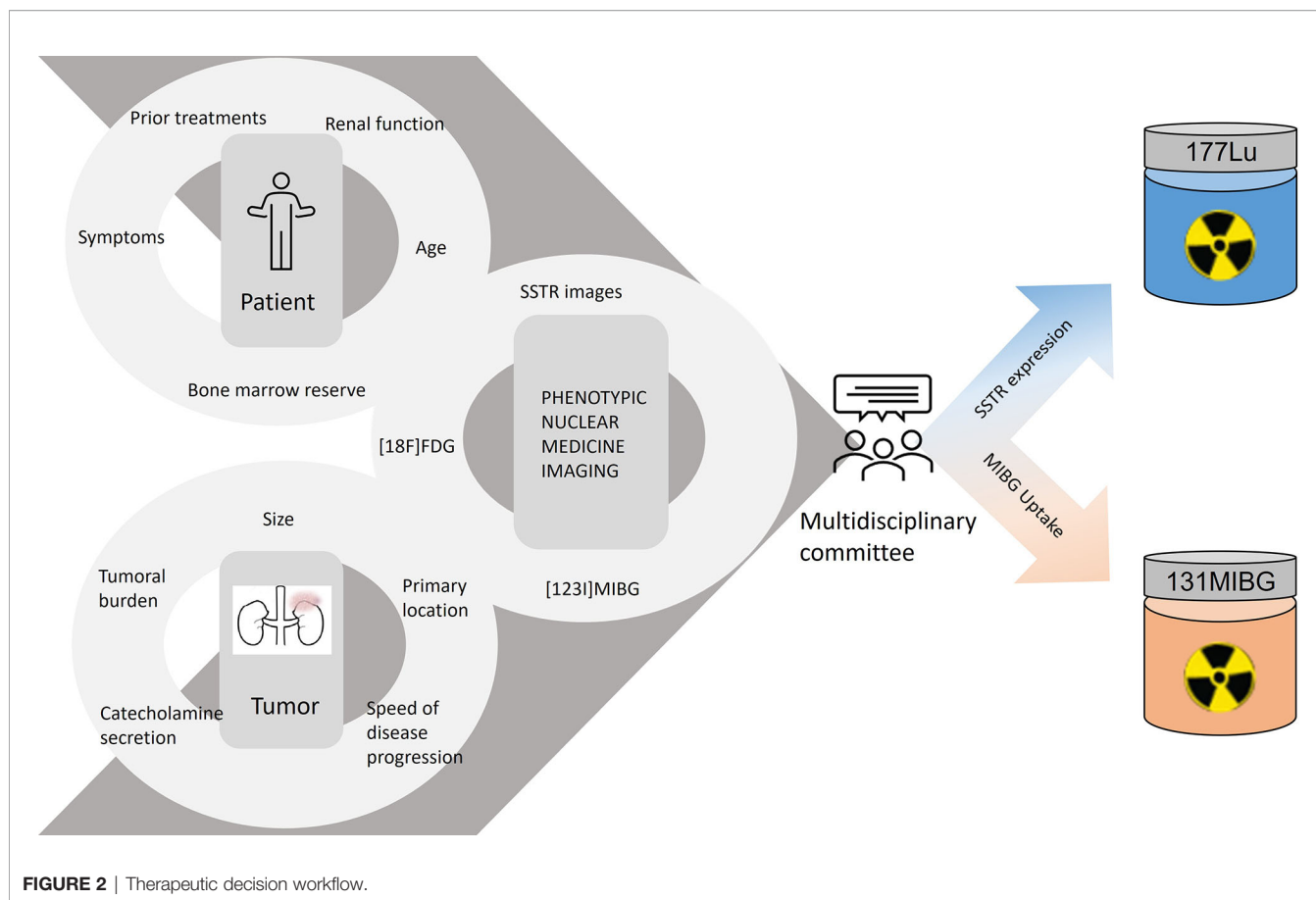


FIGURE 2 | Therapeutic decision workflow.

In patients without disease progression, SSTR molecular images were performed 3 months, 6 months, and annually after therapy. ¹⁸F]FDG was performed additionally during follow-up if needed. The tumoral lesions were morphologically characterized according to RECIST with CT or MRI.

¹³¹I-Metaiodobenzylguanidine

This arm included 8 patients (3 women) with a mean age of 45.5 years (5–77 years), displaying similar or higher uptake in ¹²³I]MIBG than the SSTR imaging scans.

In addition to the functional imaging scans, the inclusion criteria were blood test values according to the international guidelines and life expectancy over 3 months (9).

Possible drug interferences were reviewed to avoid medication interactions, including antiarrhythmics, antihypertensives, antidepressants, or sympathomimetics, as well as calcium antagonists.

A mean dose of 6.5 GBq (3.1–8.2) (SD 40.4) was administered per cycle. The lowest dose was in a pediatric patient where it was adjusted based on weight. Previous thyroid blockade with a potassium iodide solution was performed, and alpha- and beta-adrenergic blockers were administered in those patients with risk of hypertensive crisis some weeks before therapy.

Patients were admitted to the metabolic therapy unit for 4–5 days until the 1-m dose rate allowed discharge from the hospital according to local legislation. After antiemetic premedication, on

TABLE 1 | Target and purpose of the nuclear medicine scans used in this report.

| Target | Norepinephrine transporter | Somatostatin receptor | Glucose transporter | L amino acid transporter |
|--------------------|--|--|--|--|
| Functional imaging | ¹²³ I]MIBG SPECT/CT | ¹¹¹ In]n-Pentetreotide/ ^{99m} Tc]Tc-HYNIC-TOC SPECT/CT, ⁶⁸ Ga]Ga-DOTA-TOC PET/CT, ⁶⁸ Ga]Ga-DOTA-TOC PET/MR | ¹⁸ F]fludeoxyglucose PET/CT | L-6- ¹⁸ F] Fluorodopa PET/CT |
| Purpose | Diagnostic and ¹³¹ I] MIBG therapy planning | Diagnostic and ¹⁷⁷ Lu] Lu-DOTA-TATE therapy planning | Diagnostic, prognostic, and metabolic. Allows to rule out radionuclide therapy | Diagnostic and metabolic. Similarity with ¹²³ I]MIBG uptake |

the first day, slow intravenous [^{131}I]MIBG perfusion was administered during 1–4 h. In order to minimize bladder radiation, oral and intravenous hydration was encouraged.

The first response evaluation was performed most frequently after 3–6 months, except in those patients with suspected early progressive disease. Conventional imaging assessed the RECIST criteria.

RESULTS

Peptide Receptor Radionuclide Therapy Results

Out of the 9 patients, 6 were PGLs and 3 were PHEOs. Four cases were sporadic and 5 familial, out of which 4 were related to pseudohypoxic cluster (3 SDHB and 1 SDHD) and 1 NF1 mutation related to kinase signaling cluster. One patient had a locally advanced and unresectable cervical disease, and the rest had metastatic disease. Patient characteristics are summarized in **Table 2**, and the metastatic location distribution is represented in **Figure 3**.

In 7 cases, functional imaging studies revealed higher uptake in SSTR SPECT/CT or ^{68}Ga -DOTA-SSA compared to [^{123}I]MIBG (with appropriate uptake of both targets in 3 patients), and in 2 cases, only SSTR SPECT/CT was performed. In 7 patients, we acquired an additional [^{18}F]FDG scan that showed always fewer metabolic lesions than those expressing SSTRs.

Only 1 patient was treated with PRRT as first-line therapy, and the largest group was treated with second-line therapy, having previously received SSA and [^{131}I]MIBG. Two patients showing similar uptake with both SSTR imaging scans and [^{123}I]MIBG were previously treated with [^{131}I]MIBG. In these cases, the multidisciplinary committee considered PRRT as the second choice radiolabeled therapy due to the presence of radiological progression to [^{131}I]MIBG and sufficient expression of SSTRs.

The average cumulative administered radioactivity was 24.9 GBq (8.5–32.4), with a mean of 3 cycles (1–4 cycles). Two patients received only 1 cycle due to rapid progressive disease (PD). Three patients died with a mean time from treatment to death of 7 months (4–12 months). In those cases, PRRT was generally administered in a late therapeutic line (3rd to 5th line), two of them carried SDHB mutation, and all of them had bone involvement.

The overall PFS was 29 months (0–81 months) with a mean follow-up of 29.78 months (4–81 months). In the PGL group, the PFS was 25.6 months (22.4 months for the sympathetic and 42 months in the cervical parasympathetic case), and it was 35.6 months in the 3 patients with PHEO.

We observed an initial DCR of 88.8%. From patients with follow-up, initial biochemical DC was observed in 4 cases (100%), radiological DC in 9 (100%), and clinical DC in 7 (87.5%). The distribution of the primary responses is represented in **Figure 4**.

Hematological grade 1 toxicity and gastrointestinal symptoms were the most common side effects (33.3% and 22.2%, respectively). The most frequent hematological toxicities

observed were mild anemia and thrombocytopenia, which eased spontaneously and did not require the treatment dose interval to be lengthened. Within gastrointestinal symptoms, the most common were mild nausea or vomiting. Patient number 3 had a grade 3 hematological toxicity (severe thrombo and leukopenia), which did not seem directly related to PRRT but was probably induced by prior cyclophosphamide, vincristine, and dacarbazine chemotherapy (CVD). Patient number 5 presented cholecystitis after the second cycle in the context of multiple liver metastases and previous SSA treatment.

^{131}I -Metaiodobenzylguanidine Results

Eight patients were treated in this group, 3 were extra-adrenal abdominal PGLs and 5 PHEOs, 4 cases were sporadic, 2 carried an SDHB mutation, and 2 lacked genetic testing. Patient features are summarized in **Table 3**.

Three patients had previous functional imaging with [^{123}I]MIBG and [^{18}F]FDG, which were concordant. In 4 patients, SSTR SPECT/CT and [^{123}I]MIBG were performed with similar-higher avidity for [^{123}I]MIBG. One patient had undergone an [^{18}F]DOPA, an [^{18}F]FDG, and, in the context of a research project, a PET/CT-PET/MRI protocol with ^{68}Ga -DOTA-SSA. In this last patient, while the first two scans were consistent, in ^{68}Ga -DOTA-SSA, the lesions showed less uptake intensity than the liver. The PET/MRI helped us characterize cystic-necrotic lesions, especially in a doubtful lesion on CT located in the splenic capsule.

In 3 patients, [^{131}I]MIBG was the first choice systemic treatment; in another 3, it was the second option; and finally in 2 cases, it was the fourth therapeutic line.

The average cumulative administered radioactivity was 7.39 GBq (3.1–12.33). Seven patients received 1 cycle, and in one patient with wide disease extension, 2 cycles were administered at a 2-month interval.

Overall PFS was 18.5 months (0–25) with a 33.6-month follow-up (3–77 months). In the PGL group, the PFS was 27.6 months, and in the PHEO group, it was 13 months.

Three patients died, with a mean time from treatment to death of 18.33 months (1–42 months). One received CVD previously, and the other two patients were treated in a fourth-line scheme.

We observed an initial DCR of 62.5%. From patients with follow-up, initial biochemical DC was observed in 4 cases (66.6%), radiological DC in 5 (83.3%), and clinical DC in 6 (75%).

One case had a severe hypertensive event that required specific antihypertensive intravenous medication, and another one experienced high blood pressure associated with the Valsalva maneuver. We reported one gastrointestinal side effect and a grade 2 hematological toxicity adverse event with anemia and thrombocytopenia.

Overall Results

Not all the patients were candidates for both therapies. The phenotypic images, patient's profile, and tumor features selected 9 patients for PRRT and 8 for MIBG. In 5 patients, only an [^{123}I]MIBG or SSTR image was performed, and if positive, the patients

TABLE 2 | Patient characteristics in [¹⁷⁷Lu]Lu-DOTA-TATE treatment.

| Patient | Age | Gender | Primary location | Mutation | Previous treatments | Previous functional image | Metastases location | Cycles | Side effects | Biochemical response | Radiological response | Clinical response | Survival | PFS | Subsequent treatments |
|---------|-----|--------|------------------|----------|---|---|---|--------|--|----------------------|--|-------------------------------|-------------------|-----------|-----------------------|
| 1 | 38 | F | Abdominal PGL | SDHD | SSA ^a | MIBG ^d –DOPA ^e – FDG ^f + SRS ^g + | Lymph nodes, bone | 3 | No | - | PR | - | 81 months | 81 months | - |
| 2 | 20 | M | Left PHEO | NF1 | No | MIBG– FDG+ SRS ++ | Bone, lung | 3 | GI | CR ⁱ | PR | SD asymptomatic | 80 months | 80 months | - |
| 3 | 46 | F | Abdominal PGL | Sporadic | Sunitinib, SSA, CVD ^b | MIBG+, FDG+, SRS ++ | Liver, lymph nodes, bone | 1 | Hematologic grade 3 toxicity (adverse event) | PR ⁱ | SD ^k | PD | 5 months, exitus | 0 months | No |
| 4 | 50 | F | Abdominal PGL | SDHB | SSA, TMZ ^c , vertebral cementation. | FDG+, SRS +, gallium ^h + | Bone | 1 | No | - | SD | SD | 4 months, exitus | 4 months | No |
| 5 | 62 | M | Cervical PGL | SDHB | SSA | SRS+ | No (unresectable) | 4 | Acute cholecystitis after 2° cycle | PR | SD | SD asymptomatic | 42 months | 42 months | No |
| 6 | 51 | F | Left PHEO | Sporadic | SSA, bone RT. | FDG+, MIBG+/-, SRS+ | Lymph nodes, bone, lung | 4 | Hematologic grade 1 toxicity | CR | Pulmonary CR. SD in lymph nodes and bone | SD oligosymptomatic | 21 months | 21 months | No |
| 7 | 28 | M | Abdominal PGL | SDHB | CVD, vertebral cementation, SSA, pelvic RT, TMZ, ¹³¹ I-MIBG. | SRS+ FDG ++, MIBG+, Gallium++ | Lymph nodes, bone, lung | 4 | No | - | PR 10 months Afterwards PD ^j | SD 10 months Afterwards PD | 12 months, exitus | 10 months | No |
| 8 | 72 | M | Abdominal PGL | Sporadic | Bone RT, liver metastasectomy, SSA. | SRS+, MIBG+/-, Gallium++, FDG++ | Liver, lymph nodes, bone | 4 | Hematologic grade 1 toxicity | - | SD | SD | 17 months | 17 months | No |
| 9 | 45 | F | Right PHEO | Sporadic | SSA, abdominal implant resection, ¹³¹ I-MIBG. | SRS+ MIBG +Gallium++ | Liver, lymph nodes, bone, pelvic implants | 4 | Hematologic grade 1 toxicity, GI | - | SD | SD | 6 months | 6 months | No |

^aSomatostatin analogs.^bCyclophosphamide, vincristine, and dacarbazine chemotherapy.^cTemozolamide.^d[¹²³I]MIBG scintigraphy.^eL-6-[¹⁸F]fluorodopa PET/CT.^f[¹⁸F]Fludeoxyglucose PET/CT.^gSomatostatin receptor scintigraphy.^h[⁶⁸Ga]Ga-DOTA-TOC PET/CT.ⁱComplete response.^jPartial response.^kStable disease.^lProgressive disease.

++, very intense uptake; +, intense uptake; +/-, low or heterogeneous uptake; -, very low or absent uptake.

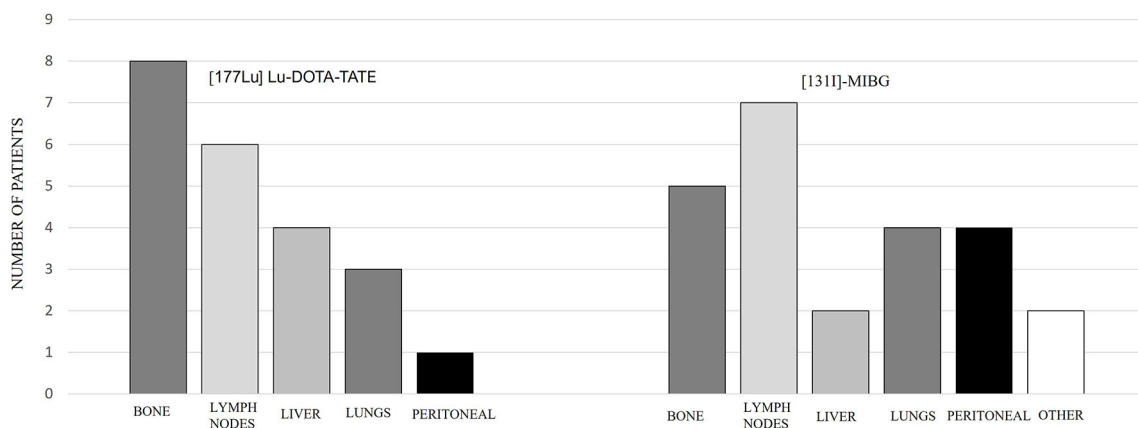


FIGURE 3 | Metastatic location in [¹⁷⁷Lu]Lu-DOTA-TATE and [¹³¹I]MIBG therapy.

were treated with the corresponding modality. In 12 patients, [¹²³I]MIBG and SSTR images were performed, and in 6 of them (50%), there was an appropriate uptake of both radiotracers (**Figure 5**). In these cases, a multidisciplinary committee decided to use that therapy with higher target uptake and/or more tailored to the clinical context as referred above. In the other 50%, we found significant heterogeneity, low or absent uptake that excluded one of the therapeutic modalities.

An association between the variables' previous treatments and PFS was observed (contingency coefficient of 0.879), with a trend to lower survival as the treatment was administered in a later line. No statistically significant differences were observed in PFS regarding primary location and therapeutic modality. A longer PFS in the PRRT modality was observed compared to [¹³¹I]MIBG, 29 vs. 18.5 months, respectively, although they did not show statistically significant differences ($p: 0.481$) (**Figure 6**).

Comparing the subgroups, the overall PFS was 26.3 months for PGLs and 21.5 months for PHEOs, with a follow-up of 35.5

and 26.9 months, respectively, with no statistical significance ($p: 0.743$) (**Figure 7**). The overall PFS with PRRT vs. [¹³¹I]MIBG was respectively 25.6 vs. 27.6 months for PGLs, and 35.6 vs. 13 months for PHEOs. The most frequent location of metastatic lesions was similar in the two therapies, predominantly in bone and lymph nodes.

DISCUSSION

Reports related to radionuclide therapy with PRRT and [¹³¹I]MIBG are usually heterogeneous case series, in procedure and data collection, with few patients and some of them not differentiating PHEO and PGL subgroups, without any clear data on PFS nor follow-up. There are often differences in [¹³¹I]MIBG treatment, particularly in patient selection and in the number of doses and cycles to be administered. The lack of consensus and a clear therapeutic guide underpin this study.

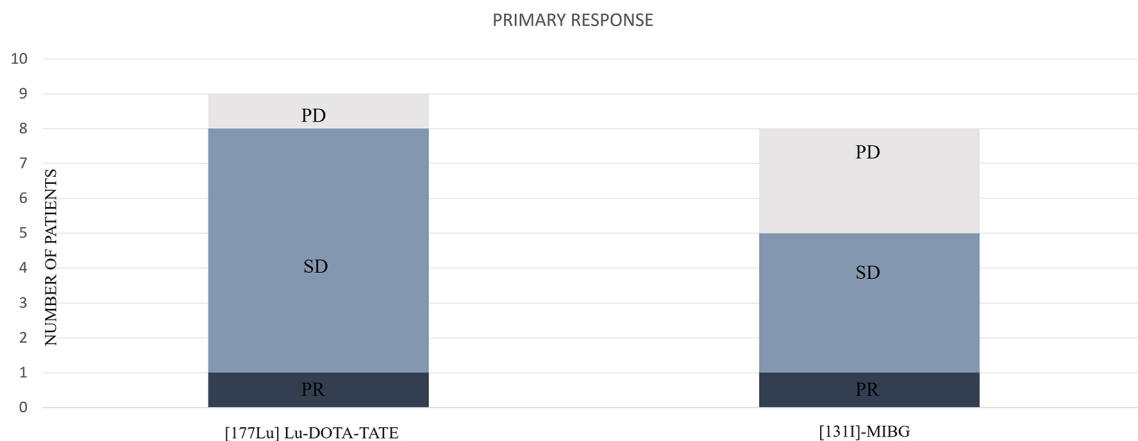


FIGURE 4 | Distribution of the primary responses according to [¹⁷⁷Lu]Lu-DOTA-TATE or [¹³¹I]MIBG. PD, progressive disease; SD, stable disease; PR, partial response.

TABLE 3 | Patient characteristics in [¹³¹I]MIBG.

| Patient | Age | Gender | Primary location | Mutation | Previous treatments | Previous functional image | Metastases location | Cycles | Side effects | Biochemical response | Radiological response | Clinical response | Survival | PFS | Subsequent treatments |
|---------|-----|--------|------------------|----------|--|--|--|--------|--|-----------------------------|-----------------------------|---|-------------------|-----------|-----------------------|
| 1 | 5 | M | Abdominal PGL | – | ¹³¹ I-MIBG 2 cycles in another center | MIBG+, FDG+ | Lymph nodes, bone | 1 | No | CR | PR | CR | 77 months | 77 months | No |
| 2 | 36 | M | Pelvic PGL | SDHB | Non specified chemotherapy. Bone thermoablation | MIBG++, FDG+ + | Lung, lymph nodes, bone, liver, abdominal implants | 2 | No | – | – | SD 6 months, Loss of clinical follow-up | 50 months | 6 months | – |
| 3 | 65 | M | Left PHEO | Sporadic | No | MIBG+, FDG+ | Lung, lymph nodes | 1 | No | SD | SD 20 months, afterwards PD | SD 20 months, afterwards PD | 49 months | 20 | CVD |
| 4 | 77 | F | Left PHEO | – | CVD | SRS+/-, MIBG++ | Lung, lymph nodes, abdominal implants | 1 | No | PD | PD | PD | 3 months, exitus | 0 | – |
| 5 | 27 | M | Abdominal PGL | SDHB | CVD, bone cementation, SSA, pelvic RT, TMZ | SRS+, MIBG+ | Bone, lymph nodes | 1 | Hypertensive crisis | PD | SD 3 months, afterwards PD | SD 6 months, afterwards PD | 32 months, exitus | 0 | PRRT 4 cycles, CVD |
| 6 | 43 | F | Right PHEO | Sporadic | SSA, abdominal implant resection | SRS+, MIBG++ | Lymph nodes, bone, abdominal implants | 1 | Hypertensive crisis with Valsalva maneuver | PR 21 months, afterwards PD | SD 21 months, afterwards PD | SD 21 months, afterwards PD | 31 months | 21 months | PRRT 4 cycles |
| 7 | 63 | F | Right PHEO | Sporadic | Liver metastasectomy nephrectomy, RT | SRS-, MIBG+ | Lymph nodes, bone, liver, kidney | 1 | No | PR | SD | SD | 24 months | 24 months | No |
| 8 | 48 | M | Left PHEO | Sporadic | CVD, CAPTEM ^a , SSA | Gallium(PET/MRI)+, MIBG+ DOPA++, FDG++ | Lung, Lymph nodes, abdominal implants, spleen | 1 | Hematologic grade 2 toxicity, GI | – | – | PD | 3 months | 0 months | No |

^aCapecitabine and temozolomide.

++, very intense uptake; +, intense uptake; +/-, low or heterogeneous uptake; –, very low or absent uptake.

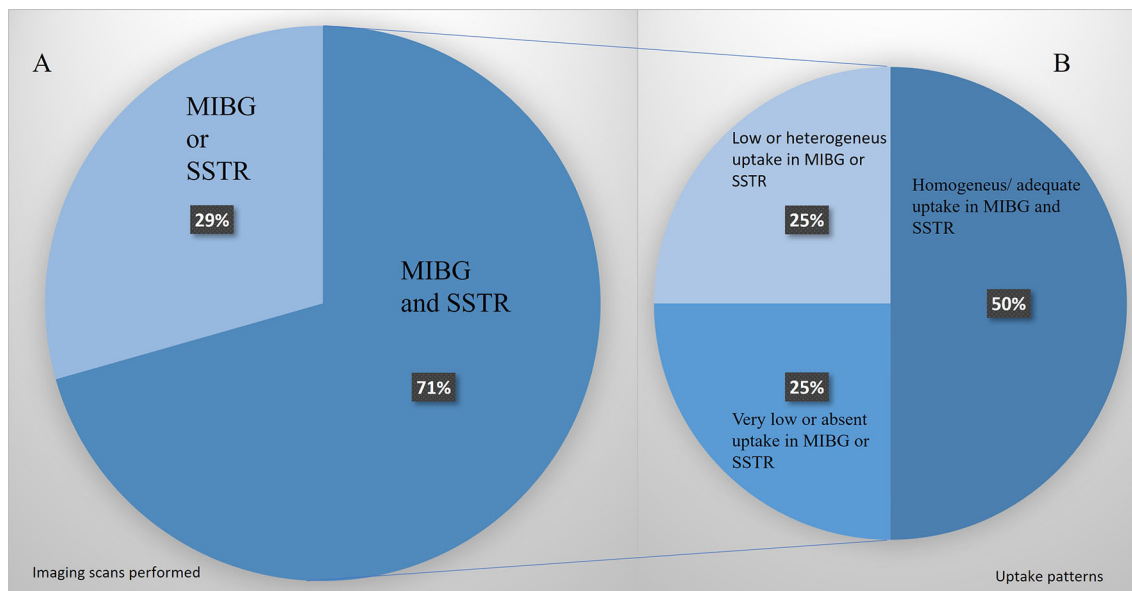


FIGURE 5 | (A) Patients' percentage assessed only by [^{123}I]MIBG or SSTR images vs. those assessed by the two image modalities. **(B)** Uptake pattern distribution in those patients studied with both image modalities.

The phenotypic imaging scans used to display the targets for radiolabeled therapy have been recently improved with novel functional imaging equipment and radiopharmaceuticals, modifying the image explorations performed over our study. The recent availability of PET/CT in the nuclear medicine departments, with higher spatial resolution than SPECT/CT or the trend of PET/MRI from the research area to the clinical application, allow to characterize higher uptakes in smaller lesions that previously went underestimated or unnoticed (10). In recent literature, Crona et al. (2017) and Nölting et al. (2019)

recommend to compare ^{68}Ga -DOTA-SSA with [^{123}I]MIBG in order to decide the best therapeutic option (11). However, in fact, these scan modalities are not fully comparable from a technical point of view and thus could lead to an underestimation of the NET expression, rejecting possible candidates to [^{131}I]MIBG. Although in the guidelines the proven tumor uptake in [^{123}I]MIBG scintigraphy is essential to plan [^{131}I]MIBG treatment, some reports lay out a high concordance degree between ^{18}F -DOPA and posttreatment distribution scintigraphy with [^{131}I]MIBG, as it happened in our patient number 8 in MIBG

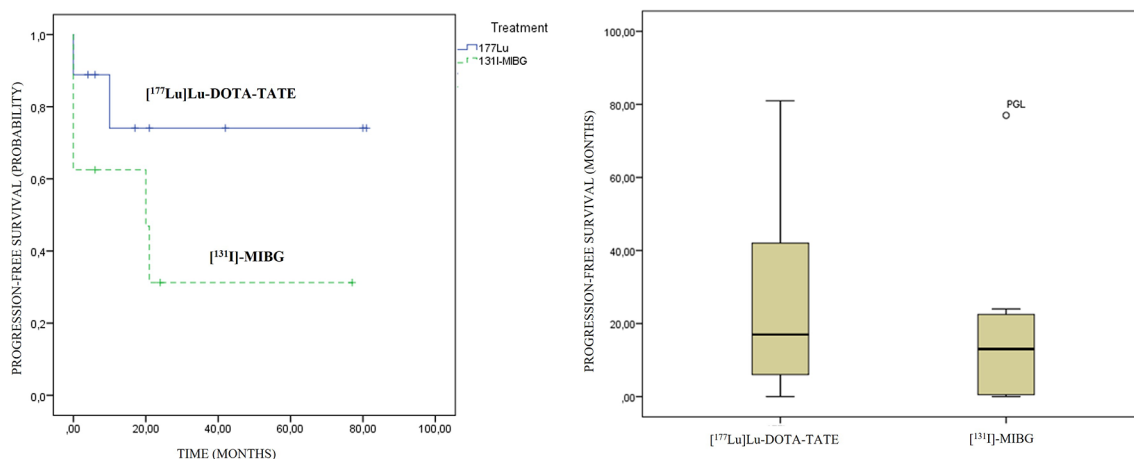


FIGURE 6 | [^{177}Lu]Lu-DOTA-TATE and [^{131}I]MIBG progression-free survival graphics. On the left side, Kaplan-Meier curves; and on the right side, box plots are presented.

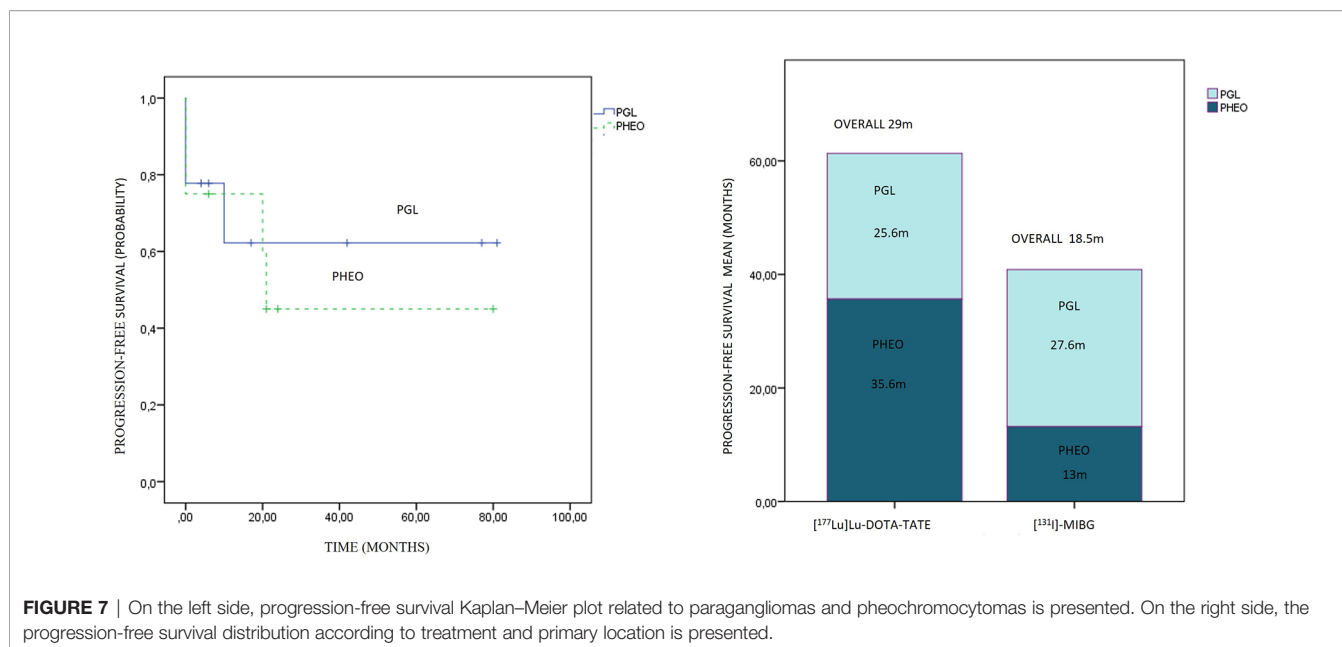


table (12–14). [^{124}I]MIBG radiotracer for PET scan is also an encouraging future option to assess the possibility of both treatments under the same conditions.

To our knowledge, this is the first published study comparing the selection and the response to treatment with full series of [^{177}Lu]Lu-DOTA-TATE and [^{131}I]MIBG in PGLs.

PRRT reported series in literature are quite homogeneous with cumulative radioactivities of between 22 and 29.6 GBq and similar PFS results to ours. Compared with studies with similar follow-up, Yadav et al. (2019) treated 25 patients with a cumulative dose of 22.8 GBq concomitantly with capecitabine, achieving a 32-month PFS with a follow-up of 30 months (15). Zandee et al. (2019) with a longer follow-up (52.5 months) obtained a 30-month PFS in 10 patients with parasympathetic PGL; 13-month PFS in the sympathetic cases; and 8, 10, and 14 months in the 3 PHEO patients (16).

In our PRRT series, there was a longer PFS in PHEOs than in PGLs. This was probably due to 3 exits in PGLs with advanced disease and high comorbidity, receiving therapy in a range from the third to fifth line.

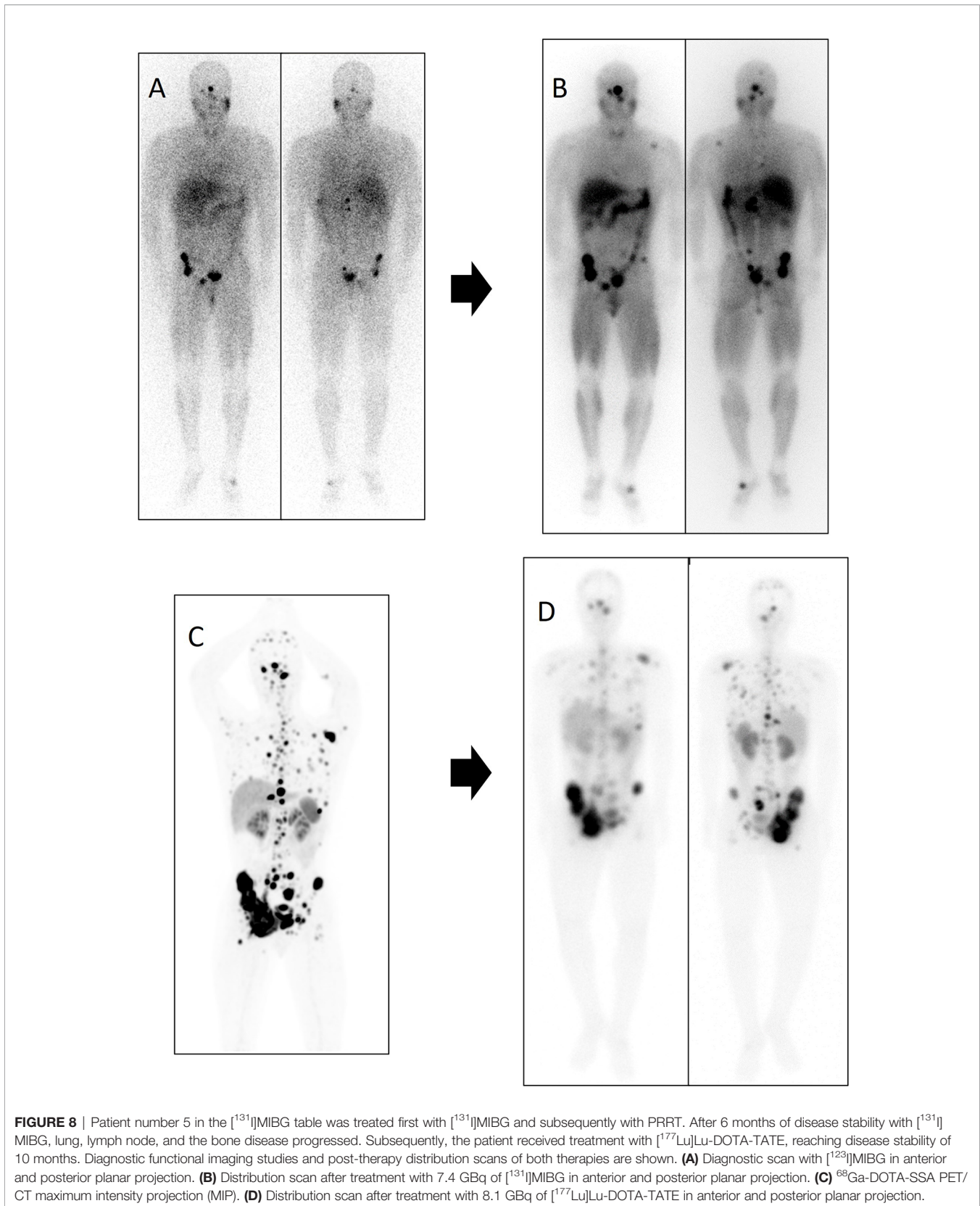
On the other hand, [^{131}I]MIBG therapy reports are quite heterogeneous in cumulative dose (between 3.7 and 39.4 GBq) and the number of cycles (1–10 cycles). It is unclear if a higher dose results in a higher tumor response or dosimetry. Castellani et al. (2010) compared two groups using intermediate vs. low cumulative dose (39.4 vs. 24.1 GBq) and observed a small variation in PFS with 30 vs. 24.92 months, respectively. They concluded that the most important difference between the groups was the shortened time to achieve a significant response (17).

Two of the studies with cumulative doses closer to ours provide a similar PFS. Shilkrot et al. (2010) with 1–4 cycles and 11.6 GBq observed a 17.5-month PFS, and Rachh et al. (2011) with 1–5 cycles and 11.8 GBq observed a PFS of 29 months (18, 19). Similar results have also been observed by

Fishbein et al. (2012) who combined 1–3 cycles of [^{131}I]MIBG and radiotherapy with an 11.26-month PFS and by Gedik et al. (2008) with 1–10 cycles of 22.2 GBq (three times more than our series) with a 28.5-month PFS. In this context, we administered a lower cumulative dose than most of those described in the literature, without any significant differences in the PFS results. Comparing by subgroups, our [^{131}I]MIBG series results agree on the recent reviews that provide a more time-sustained response to treatment for PGLs than for PHEOs (27.6 vs. 13 months) (20, 21). We also observed fewer adverse events, with only one grade 2 thrombocytopenia (12.5%), probably related to the lower dose administered (22).

In our series, sequential treatment with both radionuclides was achieved in two patients (5 and 6 of [^{131}I]MIBG series) (Figure 8). Due to a PD after [^{131}I]MIBG therapy, both received 4 cycles of PRRT. The first patient died without hematological toxicity with an overall clinical PFS of 16 months, and the second patient remains in stable disease, achieving 37-month PFS and only grade 1 hematological toxicity. These results suggest that a sequential radionuclide therapy with both modalities could be a future alternative especially in those patients with aggressive disease. Similar findings were described by Nastos et al. (2017) in two patients, one treated with [^{90}Y]Y-DOTA-TOC and the other with [^{177}Lu]Lu-DOTA-TATE, reporting grades 4 and 2 of hematological toxicity, respectively. Although our cumulative dose was in the range of those described by Nastos et al., probably in our case, the hematological toxicity was lower due to a longer delay of 10 and 12 months between both sequential treatments (23). Recently, Bushnell et al. (2021) reported a phase 1 clinical trial combining treatment with [^{90}Y]Y-DOTA-TOC and [^{131}I]MIBG in 3 patients with neuroendocrine tumors. This association allowed them to increase the dose of radiation to the tumor with an adequate margin of safety (24).

We observed a trend towards longer PFS (29 months) and DCR (88%) with PRRT and especially in PHEOs. Given that in



our series approximately half of the cases overexpressed both targets and therefore were potential candidates to both therapeutic modalities, a better approach to the treatment responses could guide the selection of the most appropriate and precise sequencing.

The current survival rates may be modified in the near future with the approval of the high-specific-activity (HSA) [¹³¹I]MIBG by the Food and Drug Administration (FDA) in 2018. In the LSA [¹³¹I]MIBG used to date, more than 99% of MIBG molecules are not labeled with ¹³¹I (“cold” MIBG). The “cold” MIBG competes with the radiolabeled molecule in the reuptake process by NETs and increases the side effects. In the HSA, the labeling process is 100–200 times more efficient, reducing side effects and competitiveness with the “cold” MIBG. [¹³¹I]MIBG (HSA) has shown in a prospective study in 68 patients with PHEOs and PGLs a sustained reduction of hypertensive medication, objective partial tumor responses of 23%, and stable disease in 69% (92% DCR). With this emerging alternative, a real intermodality agreement, in terms of spatial resolution and intensity uptake, will be required in the pretherapeutic scans (25).

Among the study limitations, the first one is that this is a retrospective case review. The PRRT and [¹³¹I]MIBG are not entirely comparable. Depending on the molecular tumor features and according to our results, at least 50% of the cases will not be candidates for both therapies. The series is small due to the low disease prevalence and does not allow to yield statistically significant differences on multiparametric tests and the survival rates in potential candidates to both treatments. The functional imaging studies are heterogeneous and have changed over time. The lack of a longer follow-up did not allow to reach the overall survival goal and to rule out late toxicities. Due to the slow progression and the disease stability periods in some patients, response to treatment could have been overestimated.

CONCLUSION

In the context of an infrequent disease with scarce therapeutic options, both [¹⁷⁷Lu]Lu-DOTA-TATE and [¹³¹I]MIBG are safe, with a promising initial DCR and a trend towards the best results in PRRT series and PHEOs. In these patients, choosing the most suitable radiolabeled treatment modality is a clinical dilemma that requires a multidisciplinary committee, and it is supported by the development of new phenotypic images. Altogether, not

only the functional imaging uptake should be evaluated. Comorbidities, patient profile, tumor features, and better response rates should also be kept in mind. The patients with the worst prognosis were those treated in later lines and with greater tumor burden. Both therapies should be studied in earlier scheme lines and with larger prospective series in order to review therapeutic selection and sequence. Although the results present limitations and the sample size and the heterogeneity of the study population do not allow to define which is the best imaging pattern to predict the response to treatment, this should be the first step to carry out a prospective study, to establish which patients would benefit from one of the two treatments and, if both can be administered, the most suitable sequence.

DATA AVAILABILITY STATEMENT

The original contributions presented in the study are included in the article/supplementary material. Further inquiries can be directed to the corresponding author.

ETHICS STATEMENT

The studies involving human participants were reviewed and approved by Hospital Universitario y Politécnico La Fe, FPNT-CEIB-04 (B). N° de registro: 2020-432-1. The patients/participants provided their written informed consent to participate in this study.

AUTHOR CONTRIBUTIONS

SP-W is the main author. MO-G, PB-A, and JM-T collaborated in the writing and revision of the article. All authors listed have made a substantial, direct, and intellectual contribution to the work and approved it for publication.

FUNDING

This study was funded by the University Hospital and Polytechnic Research Institute of Valencia, Spain.

REFERENCES

- Lenders JWM, Duh Q, Eisenhofer G, Gimenez-Roqueplo A, Grebe SKG, Murad MH, et al. Pheochromocytoma and Paraganglioma: An Endocrine Society Clinical Practice Guideline. *J Clin Endocrinol Metab* (2014) 99 (6):1915–42. doi: 10.1210/jc.2014-1498
- Neumann HPH, Young WF, Eng C. Pheochromocytoma and Paraganglioma. *New N Engl J Med* (2019) 381(6):552–65. doi: 10.1056/NEJMra1806651
- Crona J, Taieb D, Pacak K. New Perspectives on Pheochromocytoma and Paraganglioma: Toward a Molecular Classification. *Endocr Rev* (2017) 38 (6):489–515. doi: 10.1210/er.2017-00062
- Jha A, Taieb D, Carrasquillo JA, Pryma DA, Patel M, Millo C, et al. High-Specific-Activity ¹³¹I-MIBG vs ¹⁷⁷Lu-DOTATATE Targeted Radionuclide Therapy for Metastatic Pheochromocytoma and Paraganglioma. *Clin Cancer Res* (2021) 27:2989–95. doi: 10.1158/1078-0432.CCR-20-3703
- Taieb D, Hicks RJ, Hindie E, Guillet BA, Avram AM, Ghedini P, et al. European Association of Nuclear Medicine Practice Guideline/Society of Nuclear Medicine and Molecular Imaging Procedure Standard 2019 for Radionuclide Imaging of Pheochromocytoma and Paraganglioma. *Eur J Nucl Med Mol Imaging* (2019) 46 (10):2112–37. doi: 10.1007/s00259-019-04398-1
- Yip SSF, Aerts HJWL. Applications and Limitations of Radiomics. *Phys Med Biol* (2016) 61(13):R150–66. doi: 10.1088/0031-9155/61/13/R150

7. Eisenhauer EA, Therasse P, Bogaerts J, Schwartz LH, Sargent D, Ford R, et al. New Response Evaluation Criteria in Solid Tumours: Revised RECIST Guideline (Version 1.1). *Eur J Cancer* (1990) (2008) 45(2):228–47. doi: 10.1016/j.ejca.2008.10.026
8. Zaknun JJ, Bodei L, Mueller-Brand J, Pavel ME, Baum RP, Hörsch D, et al. EANM, and SNMMI Practical Guidance on Peptide Receptor Radionuclide Therapy (PRRT) in Neuroendocrine Tumours. *Eur J Nucl Med Mol Imaging* (2013) 40(5):800. doi: 10.1007/s00259-012-2330-6
9. Giammarile F, Chiti A, Lassmann M, Brans B, Flux G. EANM Procedure Guidelines for 131I-Meta-Iodobenzylguanidine (131I-MIBG) Therapy. *Eur J Nucl Med Mol Imaging* (2008) 35(5):1039–47. doi: 10.1007/s00259-008-0715-3
10. Spick C, Herrmann K, Czernin J. 18F-FDG PET/CT and PET/MRI Perform Equally Well in Cancer: Evidence From Studies on More Than 2,300 Patients. *J Nucl Med* (2016) 57(3):420–30. doi: 10.2967/jnumed.115.158808
11. Nöbling S, Ullrich M, Pietzsch J, Ziegler CG, Eisenhofer G, Grossman A, et al. Current Management of Pheochromocytoma/Paraganglioma: A Guide for the Practicing Clinician in the Era of Precision Medicine. *Cancers* (2019) 11(10):1505. doi: 10.3390/cancers11101505
12. Taieb D, Timmers HJLM, Hindie E, Guillet BA, Neumann HP, Walz MK, et al. EANM 2012 Guidelines for Radionuclide Imaging of Phaeochromocytoma and Paraganglioma. *Eur J Nucl Med Mol Imaging* (2012) 39(12):1977–95. doi: 10.1007/s00259-012-2215-8
13. Demirsoy U, Demir H, Corapcoğlu F. Bone and Lymph Node Metastases From Neuroblastoma Detected by (18)F-DOPA-PET/CT and Confirmed by Posttherapy (131)I-MIBG But Negative on Diagnostic (123)I-MIBG Scan. *Clin Nucl Med* (2014) 39(7):673. doi: 10.1097/RLU.0000000000000475
14. Piccardo A, Puntoni M, Lopci E, Conte M, Foppiani L, Sorrentino S, et al. Prognostic Value of 18F-DOPA PET/CT at the Time of Recurrence in Patients Affected by Neuroblastoma. *Eur J Nucl Med Mol Imaging* (2014) 41(6):1046. doi: 10.1007/s00259-014-2691-0
15. Yadav M, Ballal S, Bal C. Concomitant 177Lu-DOTATATE and Capecitabine Therapy in Malignant Paragangliomas. *EJNMMI* (2019) 9(1):1–10. doi: 10.1186/s13550-019-0484-y
16. Zandee WT, Feelders RA, Smit Duijzentkunst DA, Hofland J, Metselaar RM, Oldenburg RA, et al. Treatment of Inoperable or Metastatic Paragangliomas and Pheochromocytomas With Peptide Receptor Radionuclide Therapy Using 177Lu-DOTATATE. *Eur J Endocrinol* (2019) 181(1):45–53. doi: 10.1530/EJE-18-0901
17. Castellani MR, Seghezzi S, Chiesa C, Aliberti GL, Maccauro M, Seregini E, et al. (131)I-MIBG Treatment of Pheochromocytoma: Low Versus Intermediate Activity Regimens of Therapy. *Q J Nucl Med Mol Imaging* (2010) 54(1):100–13.
18. Shilkrut M, Bar-Deroma R, Bar-Sela G, Berniger A, Kuten A. Low-Dose Iodine-131 Metaiodobenzylguanidine Therapy for Patients With Malignant Pheochromocytoma and Paraganglioma Single Center Experience. *Am J Clin Oncol* (2010) 33(1):79–82. doi: 10.1097/COC.0b013e31819e2c28
19. Rachh S, Abhyankar S, Basu S. [131I]Metaiodobenzylguanidine Therapy in Neural Crest Tumors: Varying Outcome in Different Histopathologies. *Nucl Med Commun* (2011) 32(12):1201–10. doi: 10.1097/MNM.0b013e32834bad97
20. Fishbein L, Bonner L, Torigian DA, Nathanson KL, Cohen DL, Pryma D, et al. External Beam Radiation Therapy (EBRT) for Patients With Malignant Pheochromocytoma and Non-Head and -Neck Paraganglioma: Combination With 131I-MIBG. *Horm Metab Res* (2012) 44(5):405–10. doi: 10.1055/s-0032-1308992
21. Van Hulsteijn LT, Niemeijer ND, Dekkers OM, Corssmit EPM. 131I-MIBG Therapy for Malignant Paraganglioma and Phaeochromocytoma: Systematic Review and Meta-Analysis. *Clin Endocrinol* (2013) 80(4):487–501. doi: 10.1111/cen.12341
22. Gedik GK, Hoefnagel CA, Bais E, Valdes Olmos RA. [Sup.131I]-MIBG Therapy in Metastatic Phaeochromocytoma and Paraganglioma. *Eur J Nucl Med Mol Imaging* (2008) 35(4):725–33. doi: 10.1007/s00259-007-0652-6
23. Nastos K, Cheung VTF, Toumpanakis C, Navalkisoor S, Quigley A, Caplin M, et al. Peptide Receptor Radionuclide Treatment and (131)I-MIBG in the Management of Patients With Metastatic/Progressive Phaeochromocytomas and Paragangliomas. *J Surg Oncol* (2017) 115(4):425. doi: 10.1002/jso.24553
24. Bushnell DL, Bodeker KL, O'doriso TM, Madsen MT, Menda Y, Graves SA, et al. Addition Of 131i MIBG To PRRT (90y DOTATOC) For Personalized Treatment of Selected Patients With Neuroendocrine Tumors. *J Nucl Med* (2021) 62(9):1274–7. doi: 10.2967/jnumed.120.254987
25. Pryma DA, Chin BB, Noto RB, Dillon JS, Perkins S, Solnes L, et al. Efficacy and Safety of High-Specific-Activity 131I-MIBG Therapy in Patients With Advanced Pheochromocytoma or Paraganglioma. *J Nucl Med* (2019) 60(5):623–30. doi: 10.2967/jnumed.118.217463

Conflict of Interest: The authors declare that the research was conducted in the absence of any commercial or financial relationships that could be construed as a potential conflict of interest.

Publisher's Note: All claims expressed in this article are solely those of the authors and do not necessarily represent those of their affiliated organizations, or those of the publisher, the editors and the reviewers. Any product that may be evaluated in this article, or claim that may be made by its manufacturer, is not guaranteed or endorsed by the publisher.

Copyright © 2022 Prado-Wohlwend, del Olmo-García, Bello-Arques and Merino-Torres. This is an open-access article distributed under the terms of the Creative Commons Attribution License (CC BY). The use, distribution or reproduction in other forums is permitted, provided the original author(s) and the copyright owner(s) are credited and that the original publication in this journal is cited, in accordance with accepted academic practice. No use, distribution or reproduction is permitted which does not comply with these terms.